

# Ratio of cross-sections of kaons to pions produced in $pp$ collisions as a function of $\sqrt{s}$

G.I. Lykasov, A.I. Malakhov, A.A. Zaitsev

Joint Institute for Nuclear Research, Joliot Curie 6, 141980 Dubna, Russian Federation

## Abstract

A calculation of the inclusive spectra of pions and kaons produced in  $pp$  collisions as functions of their transverse momentum  $p_t$  at mid-rapidity is presented within the self-similarity approach. A satisfactory description of the data within a wide range of initial energies is presented. We focus mainly on the ratio of cross-sections of  $K^\pm$  to  $\pi^\pm$  mesons produced in  $pp$  collisions as a function of  $\sqrt{s}$ . A fast rise of this ratio, when the initial energy increases starting from the kaon production threshold up to  $\sqrt{s} \simeq 20\text{-}30$  GeV, is revealed together with its very slow increase up to LHC energies. The energy dependence of this ratio is due to the conservation laws of four-momenta and quantum numbers of the initial and produced hadrons, and to the Regge behavior of cross-sections at large energies. The more or less satisfactory agreement of these ratios with NA61-SHINE, RHIC and LHC data is demonstrated.

## 1 Introduction

The study of strange hadron production in heavy-ion collisions compared to the similar production of pions attracts the attention of theorists and experimenters. This issue became very important and intriguing after the observation of a fast rise and sharp peak in the ratio of  $K^+$  mesons to  $\pi^+$  mesons produced in central  $Pb+Pb$  and  $Au+Au$  collisions at mid-rapidity, when the initial energy  $\sqrt{s_{NN}}$  per nucleon grows from the threshold of  $K^+$  meson production up to 20-30 GeV [1, 2] and then falls down at  $\sqrt{s_{NN}} > 30$  GeV. However, the energy dependence of the  $K^-/\pi^-$  ratio in central  $Pb+Pb$  and  $Au+Au$  collisions is different, there is no peak at any  $\sqrt{s}$ , see [3] and references therein.

The  $K^+/\pi^+$  ratio in  $pp$  collisions at mid-rapidity in contrast to the similar ratio observed in  $AA$  collisions has a fast rise when the initial energy grows up to  $\sqrt{s} \simeq 20\text{-}30$  GeV and then it increases slowly with  $\sqrt{s}$ . The  $K^-/\pi^-$  ratio in  $pp$  collisions at mid-rapidity has a similar energy dependence, see [3] and references therein.

In this paper we analyze the production of kaons and pions in  $pp$  collisions at mid-rapidity and focus on ratios between their cross-sections as functions of the initial energy. Our analysis is based on the similarity of inclusive spectra of particles produced in hadron-hadron collisions, suggested in pioneering papers [4, 5, 6, 7], and on the conservation laws of four-momenta and quantum numbers [8, 9, 10, 11].

Actually, we continue to apply the approach developed in recent papers [12, 13, 14], where  $p_t$ -spectra of pions produced in  $pp$ ,  $AA$  collisions at mid-rapidity and within a wide range of initial energies were analyzed.

In [9, 11] the similarity was demonstrated at zero rapidity  $y=0$  of these spectra as functions of the similarity parameter  $\Pi$  dependent on the initial energy  $\sqrt{s}$  in the c.m.s of the colliding particles and the transverse masses  $m_{ht}$  of the produced hadrons. A simple form of inclusive spectra was used in [9, 10, 11] to describe satisfactorily the data at low values of  $m_{ht}$ . Further development of this approach was presented in our papers [12, 13, 14], where the description of  $m_{ht}$ -spectra was extended to larger values of transverse masses and initial energies up to a few TeV including contributions of both quarks and gluons to these spectra. The relationship between  $\Pi$  and the Mandelstam variables  $s, t$  was obtained in [12, 13]. Moreover, it has been shown that  $\Pi$  cannot be presented in the factorization form as a common function of  $\sqrt{s}$  and  $m_{ht}$ . The breakdown of this factorization occurs at not large initial energies  $\sqrt{s} < 10$  GeV. It is restored at larger  $\sqrt{s}$  [12, 13]. In fact, this is an advantage of the approach based on the kinematics of four-momentum velocities considered in [8, 9, 10, 11], where the parameter  $\Pi$  was obtained using the conservation laws of four-momenta and quantum numbers of initial and produced particles, and the minimization principle. At zero rapidity  $y=0$  the form for  $\Pi$  was obtained analytically [11].

In this paper we will give a brief review of the main properties of the similarity approach mentioned above and then present in detail our calculations of transverse momentum spectra of pions and kaons produced in  $pp$  collisions within a wide range of initial energies  $\sqrt{s}$ . The main focus of our paper is the theoretical analysis of ratios of cross-sections of  $K^\pm$  to  $\pi^\pm$  mesons produced in these collisions as functions of  $\sqrt{s}$  and their comparison with all the world data.

## 2 Main properties of the self-similarity approach.

The inclusive production of hadron 1 in the interaction of nucleus  $A$  with nucleus  $B$ :

$$A + B \rightarrow 1 + \dots, \quad (1)$$

is satisfied by the conservation law of four-momenta in the following form [10, 11]:

$$(N_A P_A + N_B P_B - p_1)^2 = (N_A m_0 + N_B m_0 + M)^2, \quad (2)$$

where  $N_A$  and  $N_B$  are the fractions of the four-momentum transmitted by nucleus  $A$  and nucleus  $B$ , their forms are presented in [11, 13];  $P_A$ ,  $P_B$ ,  $p_1$  are the four-momenta of nuclei  $A$  and  $B$  and particle 1, respectively;  $m_0$  is the mass of the nucleon;  $M$  is the mass of the particle providing for conservation of the baryon number, strangeness, and other quantum numbers. For  $\pi$ -mesons  $m_1 = m_\pi$  and  $M=0$ . For antinuclei  $M = m_1$  and for  $K^-$ -mesons  $M = m_1 = m_K$ ,  $m_K$  is the mass of the  $K$ -meson. For nuclear fragments  $M = -m_1$ . For  $K^+$ -mesons  $m_1 = m_K$

and  $M = m_\Lambda - m_K$ ,  $m_\Lambda$  is the mass of the  $\Lambda$ -baryon. Let us note that the isospin effects of the produced hadrons and other nuclear effects are out of this approach. Therefore, it is assumed that within the self-similarity approach there is no big difference between the inclusive spectra of  $\pi^+$  and  $\pi^-$  mesons produced in  $pp$  and  $AA$  collisions. However, there is a difference between similar spectra of  $K^+$  and  $K^-$  mesons, because the values of  $M$  are different. This is due to the conservation law of strangeness.

In [10, 11] the parameter of self-similarity is introduced in the following form:

$$\Pi = \min\left[\frac{1}{2}[(u_A N_A + u_B N_B)^2]^{1/2},\right] \quad (3)$$

where  $u_A$  and  $u_B$  are the four-velocities of nuclei  $A$  and  $B$ .

Then, the inclusive spectrum of particle 1 produced in the  $AA$  collision can be presented as a general universal function dependent on the self-similarity parameter  $\Pi$  :

$$Ed^3\sigma/dp^3 = A_A^{\alpha(N_A)} \cdot A_B^{\alpha(N_B)} \cdot F(\Pi) \quad (4)$$

where  $\alpha(N_A) = 1/3 + N_A/3$ ,  $\alpha(N_B) = 1/3 + N_B/3$  and function  $F(\Pi)$  has the following form [14]:

$$F(\Pi) = (A_q \exp(-\frac{\Pi}{C_q}) + A_g \sqrt{p_t} \phi_1(s) \exp(-\frac{\Pi}{C_g})) \sigma_{tot} \quad (5)$$

where

$$\Pi(s, m_{1t}, y) = \left\{ \frac{m_{1t}}{2m_0\delta_h} + \frac{M}{\sqrt{s}\delta_h} \right\} ch(y) \times \left\{ 1 + \sqrt{1 + \frac{M^2 - m_1^2}{(m_{1t} + 2Mm_0/\sqrt{s})^2 ch^2(y)} \delta_h} \right\}, \quad (6)$$

$\phi_1(s) = 1 - \sigma_{nd}(s)/\sigma_{tot}(s)$ , see[13, 14]. Here  $\delta_h = \left(1 - \frac{s_{th}^h}{s}\right)$ ;  $s_{th}^\pi \simeq 4m_0^2$ ;  $s_{th}^{K^+} = (m_0 + m_K + m_\Lambda)^2$ ;  $s_{th}^{K^-} = (2m_0 + 2m_K)^2$ ;  $M = m_\Lambda - m_0$ ;  $m_\Lambda = 1.115$  GeV;  $m_k = 0.494$  GeV;  $m_0 = 0.938$  GeV;

$\sigma_{tot}$ ,  $\sigma_{SD}$  and  $\sigma_{el}$  are the total cross-section, the single diffractive cross section and the elastic cross-section of  $pp$  collisions, respectively. They were taken from [18] and [19] and, together with parameters  $A_q, C_q$  and  $A_g, C_g$ , they are presented in the Appendix.

### 3 Transverse momentum spectra and integrated pion and kaon cross-sections.

For  $pp \rightarrow hX$  inclusive processes the relativistic invariant differential cross-section at small but non-zero rapidity  $y$  has the following form:

$$\begin{aligned} \rho_h(p_{ht}, y) &\equiv E_h \frac{d^3\sigma_{NN}}{d^3p_1} \equiv \frac{1}{\pi} \frac{d\sigma}{dp_{1t}^2 dy} \equiv \\ &\equiv \frac{1}{\pi} \frac{d\sigma}{dm_{1t}^2 dy} = F(\Pi(s, m_{1t}, y)), \end{aligned} \quad (7)$$

where  $F(\Pi(s, m_{1t}, y))$  and  $\Pi(s, m_{1t}, y)$  are given by Eqs. (5,6).

The production cross-section of hadron  $h$  integrated over its transverse momentum  $p_{1t}$  or transverse mass  $m_{1t}$  at zero rapidity  $y = 0$  can be presented in the following form:

$$\begin{aligned} \sigma_h(s \geq s_{th}^h, y = 0) &= \int_{p_{1t}^{min}}^{p_{1t}^{max}} \rho(s, p_{1t}, y = 0) p_{1t} dp_{1t} \equiv \\ &\equiv \sigma_{tot}(s) \int_{p_{1t}^{min}}^{p_{1t}^{max}} \exp\left(-\frac{M}{C_q \sqrt{s} \delta_h} \left\{ 1 + \sqrt{1 + \frac{M^2 - m_1^2}{(m_{1t} + 2Mm_0/\sqrt{s})^2} \delta_h} \right\}\right) (J_q + J_g) p_{1t} dp_{1t}, \end{aligned} \quad (8)$$

where

$$J_q = A_q \exp\left(-\frac{m_{1t}}{2m_0 C_q \delta_h} \times \left\{ 1 + \sqrt{1 + \frac{M^2 - m_1^2}{(m_{1t} + 2Mm_0/\sqrt{s})^2} \delta_h} \right\}\right) \quad (9)$$

and

$$\begin{aligned} J_g &= A_g \sqrt{p_{1t}} \phi_1(s) \exp\left(-\frac{m_{1t}}{2m_0 C_g \delta_h} + \frac{M(C_g - C_q)}{C_q C_g \sqrt{s} \delta_h}\right) \times \\ &\quad \left\{ 1 + \sqrt{1 + \frac{M^2 - m_1^2}{(m_{1t} + 2Mm_0/\sqrt{s})^2} \delta_h} \right\} \end{aligned} \quad (10)$$

Let us analyze qualitatively the energy behaviors of pion and kaon production cross-sections in  $pp$  collisions at zero rapidity given by Eqs. (8-10). Their  $\sqrt{s}$  dependence at not large energies is determined mainly by the factor  $\exp(-\frac{M}{C_q \sqrt{s} \delta_h})$  and factors  $\exp(-\frac{m_{1t}}{2m_0 C_q \delta_h})$ ,  $\exp(\frac{M(C_g - C_q)}{C_q C_g \sqrt{s} \delta_h})$ ,  $\exp(-\frac{m_{1t}}{2m_0 C_g \delta_h})$  entering into functions  $J_q$  and  $J_g$ . For all hadrons produced at the threshold these factors result in the zero cross section due to zero of the kinematical factor  $\delta_h = 1 - s_{th}/s$  at  $s = s_{th}$ . For  $\pi^\pm$ ,  $K^+$ ,  $K^-$  mesons the threshold energies  $\sqrt{s_{th}}$  are 2.015 GeV, 2.547 GeV and 2.86 GeV, respectively. At  $s > s_{th}$  the production cross-sections of  $K^\pm$  mesons show a fast rise due to  $M$  not being equal to zero and to an increase of  $\delta_h = 1 - s_{th}/s$ , then at  $s \gg s_{th}$

and  $s \gg M$  the energy dependence of these cross-sections changes only due to the total cross section  $\sigma_{tot}(s)$  and  $\phi_1(s) = 1 - \sigma_{nd}(s)/\sigma_{tot}(s)$  [13, 14] entering into Eq. (10). The energy dependence of the production cross-section of pions in  $pp$  collision is similar to the kaon production cross-section, however, the threshold of the pion production  $s_{th}^\pi$  is less than the kaon one  $s_{th}^{K^\pm}$ , as it is mentioned above. Therefore, the ratio of cross-sections,  $\sigma_{K^\pm}/\sigma_\pi$  exhibits a fast rise from the kaon threshold when  $\sqrt{s}$  grows due to an increase of the phase space. Then, at  $s \gg s_{th}$  this rise is broken and goes to a slow increase due, mainly, to the factors  $\phi_1(s)$  and  $\exp(\frac{M(C_g - C_q)}{C_q C_g \sqrt{s} \delta_h})$  presented in Eq. (10) because  $C_g > C_q$ , as it is shown in Table 1 of the Appendix.

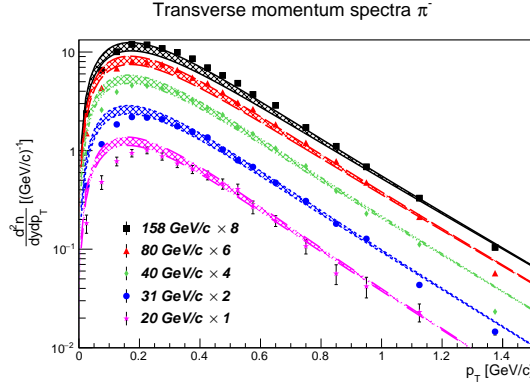


Figure 1: The  $p_t$ -spectra of  $\pi^-$  mesons produced in  $pp$  collision at  $P_{in} = 158$  GeV/c ( $\sqrt{s} = 17.28$  GeV), 80 GeV/c ( $\sqrt{s} = 12.34$  GeV), 40 GeV/c ( $\sqrt{s} = 8.77$  GeV), 31 GeV/c ( $\sqrt{s} = 7.75$  GeV), 20 GeV/c ( $\sqrt{s} = 6.27$  GeV) at mid-rapidity  $|y| < 0.2$ . The lines are our calculations, data are taken from [30], the bands are due to uncertainties in parameter  $A_q$  presented in the Appendix.

The  $p_t$ -spectra of  $\pi^-$ ,  $K^+$  and  $K^-$  mesons are sums of quark and gluon contributions including uncertainties due to the fit of data are presented in Figs. (1-3). By fitting NA61/SHINE data on  $p_t$ -spectra at mid-rapidity the parameters  $C_q, A_q, C_g$  were found to be independent of the initial energy  $\sqrt{s}$ , they depend on the kind of mesons produced,  $\pi, K^+, K^-$ . However, the parameter  $A_q$  varies a little bit at energies from 40 GeV/c up to 158 GeV/c. The uncertainties in  $p_t$ -spectra and ratios of yields,  $K^+/\pi^+$  and  $K^-/\pi^-$  are due to the uncertainties in the parameter  $A_q$ . All these parameters are presented in the Appendix. The similar spectra with quark and gluon contributions are also presented in the Appendix.

## 4 Ratio of the kaon and pion yields.

In Figs. (4,5) the respective yield ratios,  $K^+/\pi^+$  and  $K^-/\pi^-$ , are presented as functions of  $\sqrt{s}$ . From these figures one can see their fast rise from the threshold

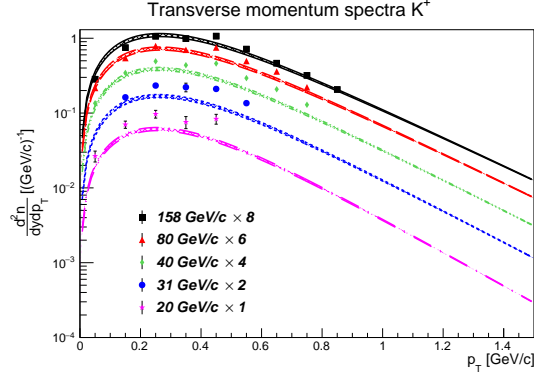


Figure 2: The  $p_t$ -spectra of  $K^+$  mesons produced in  $pp$  collision at  $P_{in} = 158$  GeV/c ( $\sqrt{s}=17.28$  GeV), 80 GeV/c ( $\sqrt{s} = 12.34$  GeV), 40 GeV/c ( $\sqrt{s} = 8.77$  GeV), 31 GeV/c ( $\sqrt{s} = 7.75$  GeV), 20 GeV/c ( $\sqrt{s} = 6.27$  GeV) at mid-rapidity  $|y| < 0.2$ . The lines are our calculations, data are taken from [30], the bands are due to uncertainties in parameter  $A_q$  presented in the Appendix.

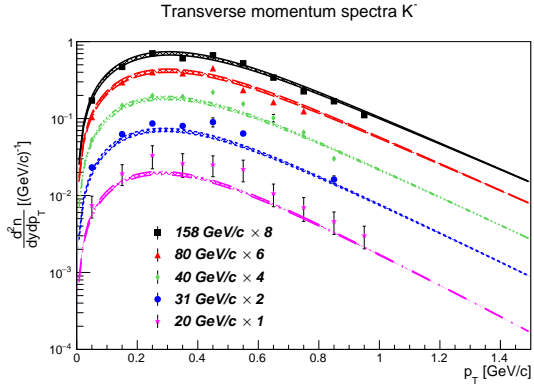


Figure 3: The  $p_t$ -spectra of  $K^-$  mesons produced in  $pp$  collision at  $P_{in} = 158$  GeV/c ( $\sqrt{s}=17.28$  GeV), 80 GeV/c ( $\sqrt{s} = 12.34$  GeV), 40 GeV/c ( $\sqrt{s} = 8.77$  GeV), 31 GeV/c ( $\sqrt{s} = 7.75$  GeV), 20 GeV/c ( $\sqrt{s} = 6.27$  GeV) at mid-rapidity  $|y| < 0.2$ . The lines are our calculations, data are taken from [30], the bands are due to uncertainties in parameter  $A_q$  presented in the Appendix.

energy of  $K^+$  or  $K^-$  production up to  $\sqrt{s} = 20\text{-}30$  GeV and their further slow increase as the energy grows.

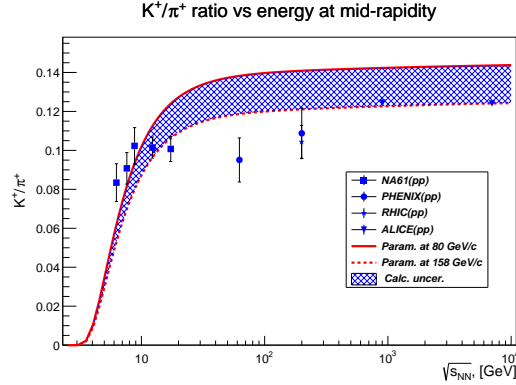


Figure 4: The ratio between yields of  $K^+$  and  $\pi^+$  mesons produced in  $pp$  collisions as a function of  $\sqrt{s}$ .

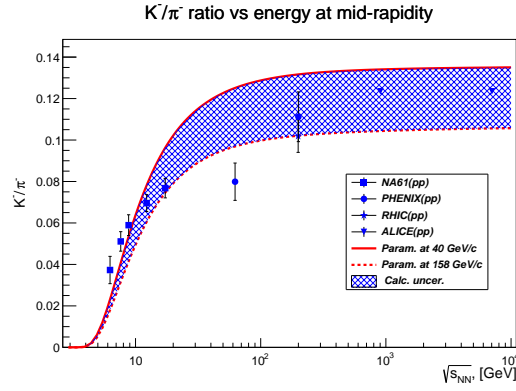


Figure 5: The ratio between yields of  $K^-$  and  $\pi^-$  mesons produced in  $pp$  collisions as a function of  $\sqrt{s}$ .

The upper line in Fig. 4 corresponds to the fit of data for  $\pi^+$  and  $K^+$  mesons at  $P_{in} = 80$  GeV/c, and the bottom line corresponds to the similar fit at  $P_{in} = 158$  GeV/c. The upper curve in Fig. 5 corresponds to the fit of data for  $\pi^-$  and  $K^-$  mesons at  $P_{in} = 40$  GeV/c and the bottom line corresponds to the similar fit at  $P_{in} = 158$  GeV/c.

## 5 Conclusion

In this paper we have applied the self-similarity approach of analysis of hadron production in  $pp$  collisions to the production of both kaons and pions in  $pp$  collisions

at mid-rapidity  $y < 0.2$  within a wide range of initial energies. The main goal of this paper is to analyze the ratio of kaon yields to those of pions, produced in  $pp$  collisions, within this approach as a function of  $\sqrt{s}$ . We have presented a self-consistent satisfactory description of the data on  $p_t$ -spectra of pions and kaons in a wide range of initial energies and not large transverse momenta. The fast rise of  $K^+/\pi^+$  and  $K^-/\pi^-$  yield ratios as functions of  $\sqrt{s}$  from the threshold energy of  $K^+$  or  $K^-$  production up to  $\sqrt{s} = 20\text{-}30$  GeV has been demonstrated as well as their further slow increase with growing energy. The energy dependence of these ratios calculated within the suggested approach results in a satisfactory description of the data presented by NA61/SHINE at  $6.27 \leq \sqrt{s} \leq 17.28$  GeV. As for the descriptions of data on  $K^\pm/\pi^\pm$  yield ratios measured by PHENIX, STAR and ALICE Collaborations, they do not contradict data taking into account the uncertainty of parameter  $A_q$  presented in Figs (4-5) as shade bands.

The physical reason of this energy dependence of the ratio of kaon yields to those of pions consists in the conservation laws of four-momenta and of reaction quantum numbers and, also, in the Regge behavior of the cross section. The conservation law of the four-momenta of initial and produced particles results in the fast rise with energy of the kaon and pion production cross-sections, when  $\sqrt{s}$  grows from the threshold energy. This is due to the factor  $\delta_h = 1 - s_{th}^h/s$  entering into the self-similarity function  $\Pi(s, m_{1t}, y)$  given by Eq.(6). A similar fast rise of the  $K^\pm/\pi^\pm$  yield ratios is also due to the factor  $\delta_h$  and to the non-zero value of  $M$  for  $K^+$  and  $K^-$  mesons that also enters into  $\Pi(s, m_{1t}, y)$ . When  $\sqrt{s} \gg \sqrt{s_{th}}$  and  $\sqrt{s} \gg M$ , the pion and kaon production cross-sections and their ratios become insensitive to factors  $\delta_h$  and  $M$ , however they are sensitive to the Regge energy behavior of cross-sections. That is why the  $K^\pm/\pi^\pm$  yield ratios exhibit two kinds of energy dependence, a fast rise, when  $\sqrt{s_{th}} < \sqrt{s} < 20\text{-}30$  GeV and a slow increase, when  $\sqrt{s} > 20\text{-}30$  GeV.

## 6 Appendix

The parameterizations of  $\sigma_{tot}$ ,  $\sigma_{SD}$  and  $\sigma_{el}$  have the following forms [18] and [19] :

$$\sigma_{tot} = (21.7(s/s_0)^{0.0808} + 56.08(s/s_0)^{-0.4525}) \text{ mb};$$

$$\sigma_{nd} = (\sigma_{tot} - \sigma_{el} - \sigma_{SD}) \text{ mb};$$

$$\sigma_{el} = (12.7 - 1.75\ln(s/s_0) + 0.14\ln^2(s/s_0)) \text{ mb}; \sigma_{SD} = (4.2 + \ln(\sqrt{s/s_0})) \text{ mb}.$$

In Fig. 6 the  $p_t$ -spectra of pions and kaons, produced in  $pp$  collisions within the initial momentum range (20-158) GeV/c, fitted by NA61/SHINE data are presented. The black dashed line corresponds to the quark contribution, the blue dash-dotted curve is the gluon contribution and the red solid line is the sum of quark and nonperturbative gluon contributions. The parameters  $A_q$ ,  $A_g$  and  $C_q$ ,  $C_g$  were found from a fit of NA61/SHINE data and are presented in Table 1.

As it is shown in [12, 13, 14], the form of inclusive pion spectra versus  $p_t$  at mid-rapidity given by Eqs. (4-6) describes satisfactorily data in a wide range of  $\sqrt{s}$



at  $p_t < 2\text{-}3$  GeV/c. Moreover, as it is shown in [15, 16] and [17], the contribution of gluons to the pion spectrum is related to the gluon distribution at low  $Q^2 = 1\text{-}2$  (GeV/c)<sup>2</sup>, the use of which results in a satisfactory description of data on hard  $pp$  processes at LHC energies and of proton structure functions at low  $x$ . Therefore, we use Eqs. (4-7) for description of data on pion  $p_t$ -spectra in  $pp$  collisions, only improving the fit of data.

As for  $K^\pm$  production in  $pp$  collisions at not large initial energies we take into account the additional contribution due to the one Reggeon exchange diagram, which has  $\sqrt{s_{th}/s}$  dependence. It leads to modification of parameter  $A_q$  in the following form  $A_q(1 + \sqrt{s_{th}/s})$ , which can be approximated by  $A_q \exp(\sqrt{s_{th}/s})$ . This correction vanishes at RHIC and LHC energies, however, it allows us to describe data at  $\sqrt{s} < 10$  GeV satisfactorily.

The parameter  $A_q$  for  $\pi$  meson production was found from the fit of NA61 data [30, 3] at initial energies  $P_{in} = 40\text{-}158$  GeV/c. It is very close to the value of  $A_q$  obtained in [12, 13, 14]. For  $K^+$  production the value of  $A_q$  was found from the fit of NA61 data at  $P_{in} = 80$  GeV/c and  $P_{in} = 158$  GeV/c. For  $K^-$   $A_q$  was found from a fit of NA61 data at  $P_{in} = 40$  GeV/c and  $P_{in} = 158$  GeV/c. Other parameters  $A_g, C_q$  and  $C_g$  were fixed from a fit of the NA61 data at  $P_{in} = 80$  GeV/c and they do not depend on other initial energies.

Table 1: Table of parameters found from the fit of NA61/SHINE data [30].

$pp \rightarrow hX$	$\pi$			$K^+$		$K^-$	
$\sqrt{s_{pp}}$ , GeV	17.3	12.3	8.8	17.3	12.3	17.3	8.8
$P$ , GeV/c	158	80	40	158	80	158	40
$A_q$	3.361	3.063	2.688	0.9925	1.152	1.951	2.219
$C_q$	0.147			0.148		0.148	
$A_g$	1.788			0.7726		0.629	
$C_g$	0.22			0.2066		0.2271	

### Acknowledgements.

We are very grateful to K.A. Bugaev, M. Gumberidze, M. Gazdzicki, R. Holzmann, S. Pulawski, G. Pontecorvo for extremely helpful discussions.

## References

- [1] S.V. Afanasiev, et al., (NA49 Collaboration) Phys.Rev.C **66**, 054902 (2002).
- [2] C. Alt, et al., (NA49 Collaboration) Phys.Rev.C **77**, 024903 (2008).
- [3] A. Aduszkiewicz, et al., (NA49 Collaboration) Phys.Rev.C **102**, 011901(R) (2020).

- [4] E. Fermi, Phys. Rev. **92**, 452 (1953)
- [5] I. Ya. Pomeranchuk, Izv. Dokl. Akad. Nauk Ser.Fiz. **78**, 889 (1951).
- [6] L.D. Landau, Izv. Akad. Nauk Ser. Fiz. **17**, 51 (1953).
- [7] R. Hagedorn, Supplemento al Nuovo Cimento **3**, 147 (1965).
- [8] A.M. Baldin, L.A. Didenko, Fortsch.Phys. **38**, 261 (1990).
- [9] A.M. Baldin, A.I. Malakhov, and A. N. Sissakian, Phys. Part. Nucl. **29** (Suppl. 1), 4 (2001).
- [10] A. M.Baldin, A. A. Baldin. Phys. Particles and Nuclei, **29** No3, 232 (1998).
- [11] A.M. Baldin, A.I. Malakhov. JINR Rapid Communications, No.1(87)-98, pp.5-12 (1998).
- [12] D.A. Artemenkov, G.I. Lykasov, A.I. Malakhov, Int.J.Mod.Phys. **A30** (2015) 1550127.
- [13] G.I. Lykasov, A.I. Malakhov, Eur. Phys. J. A **54**, 187 (2018).
- [14] A.I. Malakhov, G.I. Lykasov, Eur. Phys. J. A **56**, 114 (2020).
- [15] A.A. Grinyuk, G.I. Lykasov, A.V. Lipatov, N.P. Zotov, Phys.Rev. **D87**, 074017 (2013).
- [16] A.V. Lipatov, G.I. Lykasov, N.P. Zotov, Phys.Rev. **D89**, 014001 (2014).
- [17] A.M. Abdulov, H. Jung, A.V. Lipatov, G.I. Lykasov, M.A. Malyshev, Phys.Rev. **D98**, 054010 (2018).
- [18] N. Cartiglia, arXiv:1305.6131 [hep-ex].
- [19] S.H. Stark, Eur.Phys.J. (Web of Conf.) **141** 03007 (2017).
- [20] E. Schnedermann, J. Sollfrank, U. Heinz, Phys.Rev.C48,2462 (1993).
- [21] G. Wilk, Z. Wlodarczyk, Phys.Lett. **84**, 2770 (2000).
- [22] K.A. Bugaev, J.Phys.G:Nucl.Phys., **28**, 1981 (2002).
- [23] K.A. Bugaev, M. Gadzicki, M.I. Gorenstein, Phys.Lett. B**544**, 127 (2002).
- [24] J. Cleymans, G.I. Lykasov, A.S. Parvan, et al., Phys.Lett. B **723**, 351 (2013).
- [25] J.L. Kley, et al., E895 Collaboration, Phys.Rev. C **68**, 054905 (2003).
- [26] J. Cleymans, J. Struempfer, L. Tirko, Phys.Rev. C **78**, 017901 (2008).

- [27] N. Abgrall, et al., NA61/SHINE Collaboration, Eur. Phys. J. C **74**, 2794 (2014).
- [28] K.A. Ter-Martirosyan, Sov.J.Nucl.Phys., **44**, (1986) 817.
- [29] A.A. Grinyuk, G.I. Lykasov, A.V. Lipatov, N.P. Zotov, Phys.Rev. **D87**, (2013) 074017.
- [30] A.Adiszkiewicz, *et al.*, (NA61/SHINE Collaboration) Eur.Phys.J.**C77**, 671 (2017).
- [31] B.I. Abelev *et al.*, (STAR Collaboration), Phys. Rev. **C75**, 064901 (2007).
- [32] B.I. Abelev *et al.*, (STAR Collaboration), Phys.Rev.Lett., **97**, 152301 (2006).
- [33] K. Aamodt, *et al.*, (ALICE Collaboration), Eur. Phys. J. C **71** 1655 (2011).
- [34] K. Aamodt, *et al.*, (ALICE Collaboration), Phys. Lett. **B693**, 53 (2010).
- [35] K. Aamodt, *et al.*, (ALICE Collaboration), Phys. Rev. **D82**, 052001 (2010).
- [36] K. Aamodt, *et al.*, (ALICE Collaboration), Phys. Rev. **C88**, 044910 (2013).
- [37] E. Kaptur, PoS **CPOD2014**, (2015) 053
- [38] M. Lewicki, arXiv:1612.01334 [hep-ex].

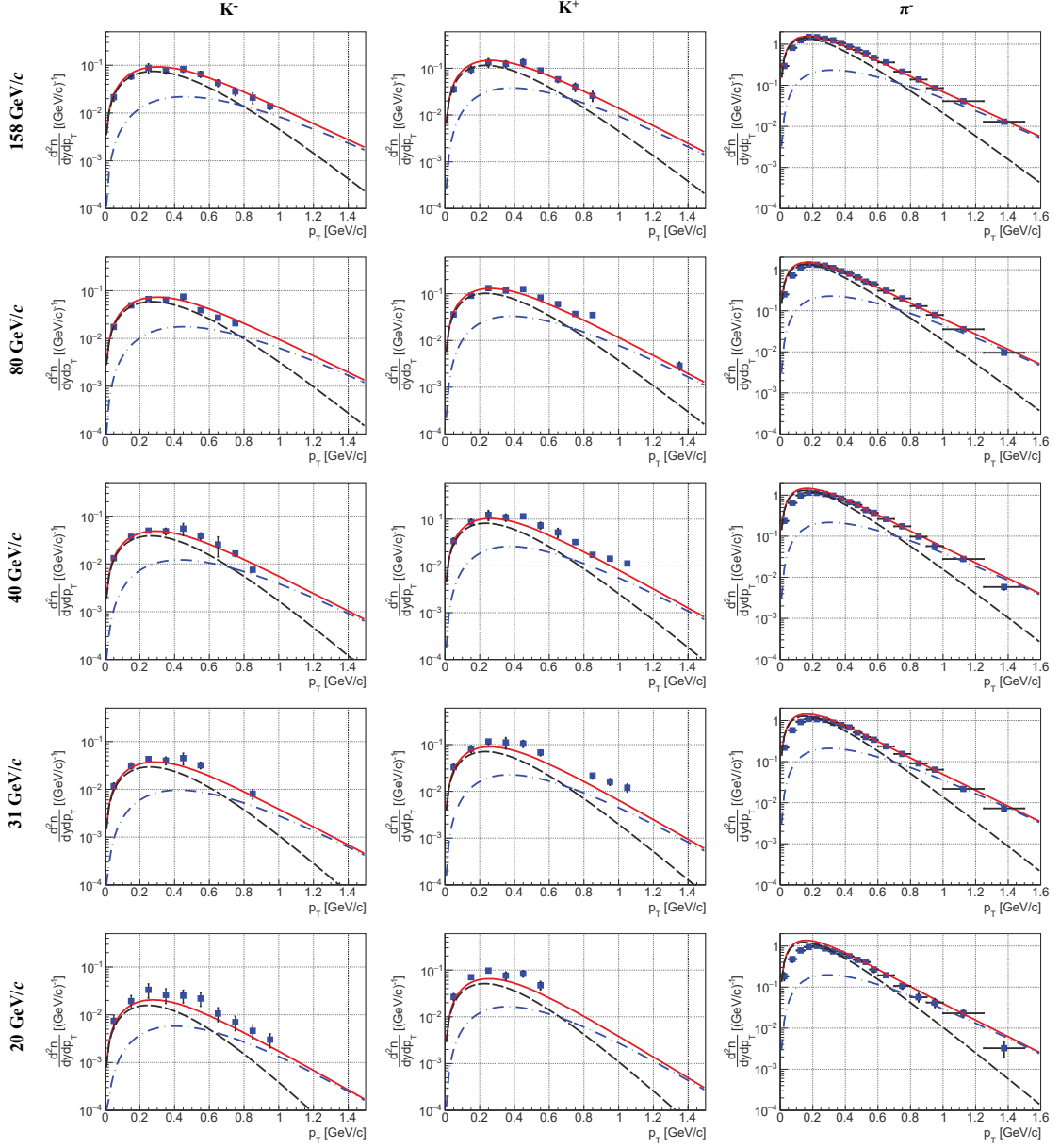


Figure 6: The  $p_t$  spectra of  $\pi^-$ ,  $K^+$  and  $K^-$  mesons produced at  $y \approx 0$  in inelastic  $pp$  interactions at SPS energies  $\sqrt{s} = 6.3 - 17.3$  GeV or  $P_{in} = 20-158$  GeV/c. Data are taken from [30].